Hindawi
Advances in Civil Engineering
Volume 2024, Article ID 6232941, 14 pages
https://doi.org/10.1155/2024/6232941

Research Article

Optimal Mix Design and Mechanical Properties of Rapid-Hardening Foam Concrete

Yuan Liu,[1] Danni Zhao,[2] Ruibo Yin,[2] Qiang Li,[2] Xiong Wu,[2] Xianglong Zeng,[2] Wei Qiao,[2] and Jiangbo Xu[2]

[1]*Rocket Force University of Engineering, Xi' an 710000, China*
[2]*School of Highway, Chang'an University, Xi' an 710064, China*

Correspondence should be addressed to Jiangbo Xu; xujiangbo@yeah.net

Received 5 January 2024; Revised 31 January 2024; Accepted 19 February 2024; Published 20 March 2024

Academic Editor: Salar Farahmand-Tabar

This paper conducts compressive strength tests on foam concrete prepared under four factors and three levels through the design of orthogonal experiments. It delves into the phase change rules of the load–displacement curves obtained under various mix proportions. Furthermore, based on the 1-day and 3-day compressive strength values, the study explores different mix proportion results using range analysis and variance analysis methods, thereby determining the optimal mix proportion that can satisfy the maximum 1-day and 3-day compressive strength values. The results indicate that the compression process of rapid-hardening foam concrete includes four stages: initial compaction stage, elastic stage, yielding stage, and plateau stage, with each stage having different causes. Additionally, the sensitivity sequence of factors affecting the 1-day and 3-day compressive strength of rapid-hardening foam concrete is respectively rapid sulfoaluminate cement (α) > water-reducing agent content (δ) > foam content (β) > water-cement ratio (γ) and rapid sulfoaluminate cement (α) > water-cement ratio (γ) > foam content (β) > water-reducing agent content (δ). With 100% sulfoaluminate cement content, the 1-day and 3-day compressive strength values can reach 1.7054 and 2.5471 MPa, respectively, which are 13 times and 7 times the minimum values of 1-day and 3-day compressive strength under other admixtures. The analysis shows that the content of rapid sulfoaluminate cement has the most significant effect on the 1-day and 3-day compressive strength of rapid-hardening foam concrete, with foam content having the least impact on 1-day compressive strength and water-reducing agent content having the least impact on 3-day compressive strength. By integrating range analysis and variance analysis, the optimal mix proportion that simultaneously satisfies the maximum 1-day and 3-day compressive strength is determined to be 100% content of rapid-hardening sulfoaluminate cement, 4% foam content, 0.55% cement ratio, and 0.12% admixture content. Overall, this study provides theoretical support for the research and development of new rapid-hardening foam concrete materials and has significant practical implications for the emergency repair and construction of infrastructure projects.

1. Introduction

Transportation is the forerunner of economic development and a vital reliance for strengthening national defense, holding dual significance in both economic and military aspects. In transportation infrastructure projects, urgent repairs and construction are often required for the transportation facilities [1]. Due to its convenient construction and outstanding properties, foam concrete has been widely applied in various fields. Additionally, the excellent performance exhibited by foam concrete has earned favor and popularity among researchers and professionals in the engineering domain [2].

At present, the research on foam concrete mainly focuses on two aspects: ratio design and material performance. In terms of material ratio design, Zheng et al. [3] established a 3D model of a foam concrete mixer through numerical simulation and studied the influence of different parameters on the mixing of cement and foam, providing a reference for designing new mixing equipment. Xiong et al. [4] used $Ca(OH)_2$ as a stabilizer to improve foam stability, thereby enhancing the compressive strength of foam concrete. Dang et al. [5] prepared foam by using three types of foaming agents and studied the early stability behavior of the three types of foam in an alkaline environment and alkali-activated foam concrete to prepare foam concrete with better early stability. Li et al. [6] established a predictive model for mechanical properties using response surface methodology and optimized the parameters of carbon nanotube-reinforced fly ash foam concrete. Uniaxial compression tests were combined with the digital speckle correlation technique to study its load-deformation characteristics. Hao et al. [7] studied the optimal mix proportion of foam concrete through orthogonal experiments and established the relationship between the mechanical properties of foam concrete and influencing factors. The microstructure of foam concrete was observed using scanning electron microscopy (SEM). Xiao et al. [8], based on the forces acting on foam, analyzed the results of pore diameter distribution, collapse depth, and density deviation to establish the influence of foam characteristics and paste viscosity on its stability, subsequently developing a theoretical model. In addition, in terms of material performance, Gao et al. [9] conducted in-depth research on foam concrete's pore structure and thermal conductivity with different densities using X-CT technology and simulation. Liu et al. [10] studied the mechanical and energy absorption properties of thin-walled multi-cell square tubes, rotating thin-walled multi-cell square tubes, and RSTFC (rotating thin-walled multi-cell square tubes with foam concrete filler) through compression experiments and explored the impact of four factors on the mechanical and energy absorption properties of RSTFC using validated models. Liu et al. [11] explored the failure patterns and stress–strain characteristics of specimens under three factors: con-fining pressure, high-temperature treatment, and loading rate, through triaxial compression tests. Gencel et al. [12] investigated the effects of varying contents of basalt fibers and silica fume on the physico-mechanical properties of foam concrete, leading to the development of a highly durable foam concrete. Ma and Chen [13] studied the modified effect of adding silica fume to foam concrete on its structure and mechanical properties, determining the optimal dosage for the best improvement effect. Li et al. [14] investigated the physical and mechanical properties of sulfoaluminate cement-based foamed concrete prepared with different mix ratios, achieving a formulation that exhibits excellent physical and mechanical properties. Jhatial, Ashfaque et al. [15] investigated the impact of incorporating Palm Oil Fuel Ash, Eggshell Powder, and reinforced polypropylene fibers on the strength and carbon dioxide emissions of ternary binder foamed concrete. Tang et al. [16] investigated the effects on physical, chemical corrosion, and mechanical properties of plain recycled foamed concrete (RFC), polyethylene terephthalate (PET) fiber reinforced RFC, and recycled PET fiber reinforced RFC, identifying the optimal mix proportions. Additionally, SEM and X-ray diffraction (XRD) analyses were conducted to explore the improvement of the micropore structure in RFC. Hang and Yang [17] studied the compressive strength, thermal conductivity, and water absorption of foam concrete with single-fly ash, slag powder, and combined-fly ash and slag powder. Based on the above analysis, it is evident that foam concrete exhibits relatively lower early strength by changing the amount of a single admixture. This limitation hinders its extensive use in urgent repair and construction scenarios. Currently, research on foam concrete has focused solely on timely improving its early strength, with no attempts made towards rapid-hardening foam concrete.

Table 1: Performance indicators of foaming agent.

Foaming multiple	1-hr settlement (mm)	1-hr water loss rate (%)
33.5	1.20	61.6

In summary, rapid-hardening foam concrete has the advantages of short setting and hardening time, high early strength, excellent workability, convenient preparation, outstanding thermal insulation, shock absorption and energy dissipation, and reduced construction periods. Its applications include repairing road collapses to speed up the repair process; repairing airport craters to prevent delays in military operations; reinforcing areas affected by mudslides for rapid post-disaster rescue and reconstruction; and regular maintenance and repair of urban roads, reducing construction time while ensuring road quality and smoothness. Thus, rapid-hardening foam concrete has tremendous potential for development in the field of rapid repair and emergency protection. So, conducting research on the preparation and properties of rapid-hardening foam concrete has significant engineering significance and economic benefits.

2. Materials and Methods

2.1. Test Materials. Silicate cement P · II42.5R, produced by Nanjing Cement Plant Co., Ltd., was used for the silicate cement. Rapid-hardening calcium aluminate cement P · II42.5R, produced by Zhengzhou Wanglou Cement Industry Co., Ltd., with a specific surface area of 480 m^2/kg and a pH value of 9 was used for the rapid-hardening cement. The admixture was provided by Shandong Yousuo Chemical Technology Co., Ltd., and the foaming agent was a high molecular composite foaming agent from Weihai Zhongsheng New Building Materials Co., Ltd., diluted 40 times, with specific performance indicators as shown in Table 1.

2.2. Experimental Scheme. The orthogonal experiment method is commonly used in multi-factor experimental design [18]. It conducts experiments by selecting representative specimen points, which have the characteristics of uniform and neat distribution. The orthogonal experimental design is the main method of partial factor design, featuring high efficiency, as it ensures the uniform distribution of test points and reduces the number of experiments [18].

By designing orthogonal experiments, the influence of the four factors, namely rapid-hardening calcium aluminate cement content (α), foam content (β), water-cement ratio (γ), and admixture content (δ) on the mechanical properties of the foam concrete, will be explored, and the influence rules of its mechanical properties will be revealed. Each factor was set at three levels, and according to the orthogonal experimental design table, a total of nine groups of experiments were conducted. The orthogonal experimental plan is shown in Table 2.

Table 2: Factor levels of the orthogonal experimental design.

Factor levels	Fast-hardening sulfoaluminate cement dosage (factor α) (%)	Foam content (factor β) (%)	Water-to-cement ratio (factor γ)	Superplasticizer content (factor δ) (%)
1	100	3.8	0.5	0.1
2	50	4	0.55	0.12
3	0	4.2	0.6	0.14

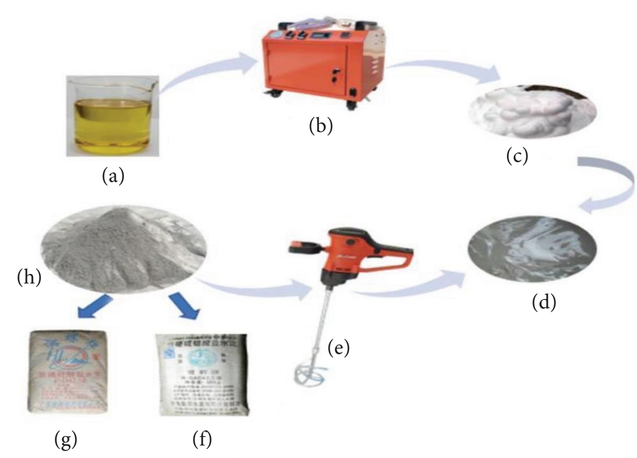

Figure 1: Preparation process of foam concrete slurry. (a) Foaming agent stock solution. (b) Foaming machine. (c) Foam. (d) Cement paste. (e) Handheld blender. (f) Cement. (g) Silicate cement. (h) Rapid-hardening sulfoaluminate cement.

The orthogonal experimental results were processed using the range analysis and analysis of variance methods. The range analysis process includes calculating the total sum K values for each factor at each level and computing the R-value, which is the difference between the maximum and minimum K values for each factor. The analysis of variance process involves first calculating the sum of squares, and based on that, calculating the mean square by dividing the sum of squares by the degrees of freedom. Then, the F-value and significance level are calculated using the respective formulas, followed by comparative analysis.

2.3. Preparation of Specimens and Performance Testing. Based on the orthogonal experimental plan, the preparation of foam concrete specimens was carried out. Firstly, referring to the mix proportion design section in Chapter 2.4 of "Foam Concrete," the mix proportions of foam concrete were calculated, and a certain amount of cement, admixture, water, and foaming agent was weighed according to these proportions [19]. All dry materials were placed in a foam concrete mixer for uniform mixing, and the foaming machine was used to produce foam. After foam preparation, the foam was mixed with the mortar for 3 min until it was evenly mixed and then poured into molds with dimensions of 100 mm × 100 mm × 100 mm. For silicate cement, the molds were demolded after 24 hr of curing; for rapid-hardening calcium aluminate cement, the molds were demolded after 1 hr of curing. Finally, the specimens are placed in a constant temperature and humidity standard curing box for curing, as shown in Figure 1. The rapid-hardening foam concrete specimens after preparation are shown in Figure 2.

Figure 2: Prepared rapid-hardening foam concrete specimens.

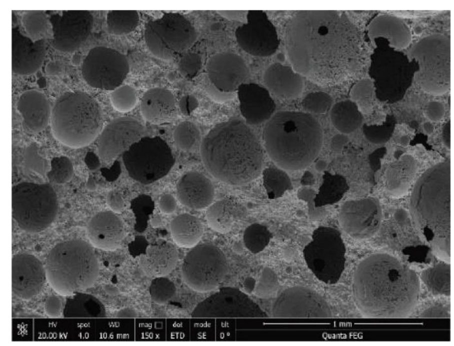

Figure 3: Structural morphology of foamed concrete magnified by 150 times.

After the specimens were prepared, a universal testing machine was used to apply a load along the axial direction of the specimen at a loading rate of 0.05 mm/s under displacement control until the specimen was crushed and the loading was stopped, thereby obtaining the 1-day and 3-day load–displacement curves of the specimens. Three parallel tests were performed for each group of mixed proportions.

3. Results, Analysis, and Discussion

3.1. Analysis of Microscopic Structural Morphology. SEM experiments were conducted to observe the microstructure of the foam concrete in detail. Figure 3 shows the microstructure of the magnified 150 times of the foam concrete specimen. It can be observed that there were many evenly distributed pores inside the foam concrete, with relatively consistent pore sizes and spacings. Figure 4 shows the pore matrix part of the foam concrete magnified 5,000 times by

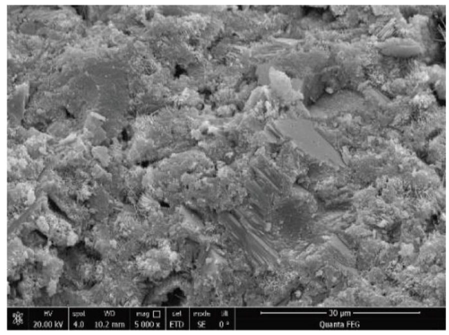

FIGURE 4: Structural morphology of foam concrete pore matrix enlarged by 5,000 times.

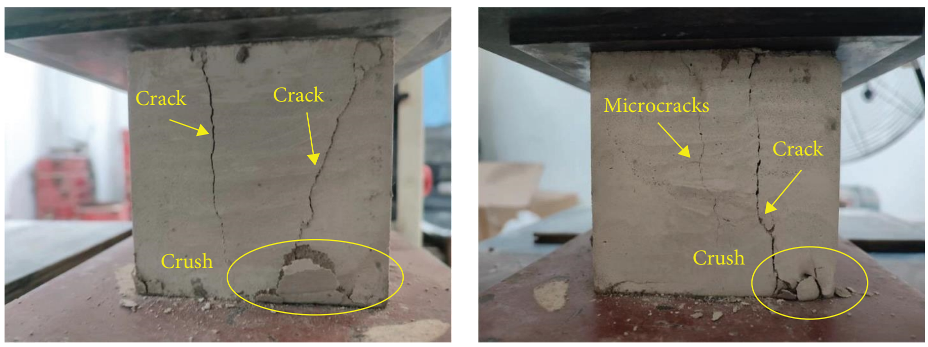

(a) (b)

FIGURE 5: Compression testing the final state of rapid-hardening foam concretes. (a) 1d compressive test; (b) 3d compressive test.

SEM. It can be observed that the connection of the pore matrix part was relatively loose, and there were slight crack phenomena. Further analysis revealed that these fine cracks were caused by the drying and self-shrinkage effects of the specimens. Through the observation of the microstructure of the foam concrete, it can be deduced that its matrix structure was loose, with low strength, and the pores had initial defects and damage, all of which led to the decrease in the mechanical properties of the foam concrete.

3.2. Analysis of Compressive Strength Test Results. To explore the mechanical properties of the rapid-hardening foam concrete specimens prepared in this study, uniaxial compression tests were carried out on each group of rapid-hardening foam concrete specimens. The compression testing final state of rapid-hardening foam concrete is shown in Figure 5. Due to the similar compression testing processes of different groups of specimens, the typical compression testing process is presented here as a representative. Meanwhile, it can be clearly seen from Figure 5 that compared with the rapid-hardening foam concrete cured for 1 day, the rapid-hardening foam concrete cured for 3 days under the same compression condition has only a few cracks on its surface, and only a little crush at the bottom, and its structure is still relatively complete. Additionally, compared with ordinary foam concrete [20, 21], the performance of the rapid-hardening foam concrete prepared in this paper after curing for around 1–3 days has basically reached the performance of its curing for about 14–28 days.

Besides, Figures 6 and 7 show the load–displacement curves of foam concrete specimens prepared with four different influencing factors (α, β, γ, δ) obtained from uniaxial compression tests at different ages. Under uniaxial compression, the compressive strength of foam concrete at different ages is shown in Table 3. In addition, due to the existence of accidental errors, three parallel specimens were prepared under each mix ratio, and the average peak load of the load–displacement curve of the three specimens prepared under each mix ratio was taken to calculate the compressive strength value under each mix ratio. The calculation results are shown in Table 4 and 5. From Table 4 to 5, it can be seen that there is some error in the load–displacement curves of the three specimens under each ratio, but the error is mostly less than 10%, which is within the allowable error range. Therefore, the average value calculated from the three specimens can be taken as the final compressive strength value.

From Figures 6 and 7, it can be observed that the load–displacement curves of foam concrete considering the four influencing factors all exhibit distinct stages. After a detailed analysis of the curves, the compression process of foam concrete can be divided into four stages, namely the initial compaction stage, compacted stage, yield stage, and platform stage; the above results are consistent with the conclusions drawn by Yuan et al. [20]. The initial compaction stage generally occurs in the early loading period of foam concrete. When subjected to external loads, foam concrete begins to deform, resulting in a rapid increase in displacement with the increasing load. The reason is that at this stage,

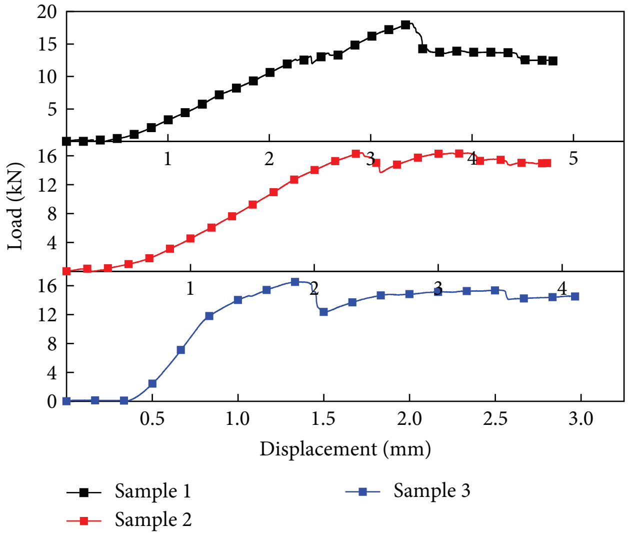

(a)

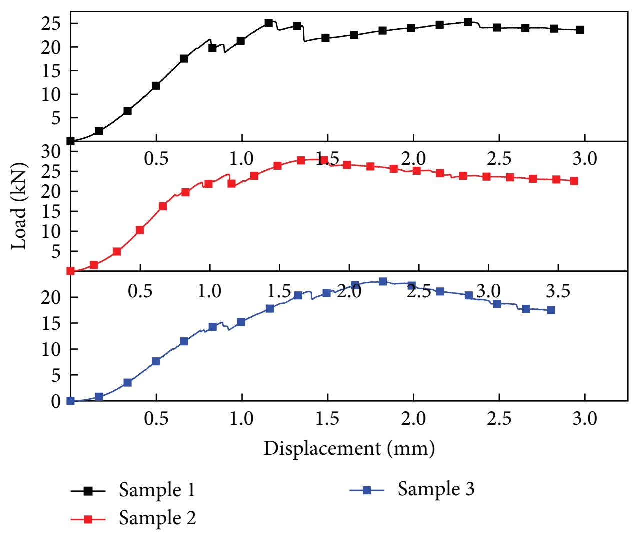

(b)

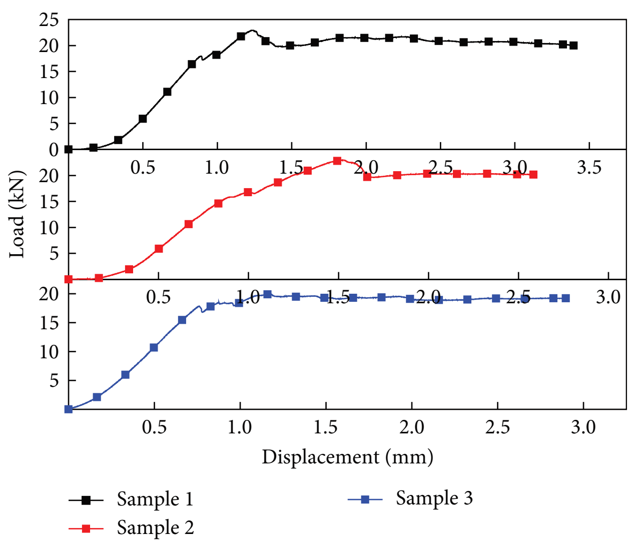

(c)

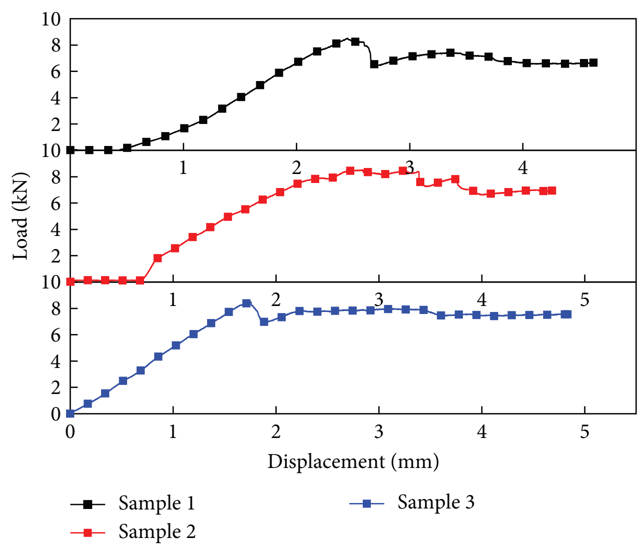

(d)

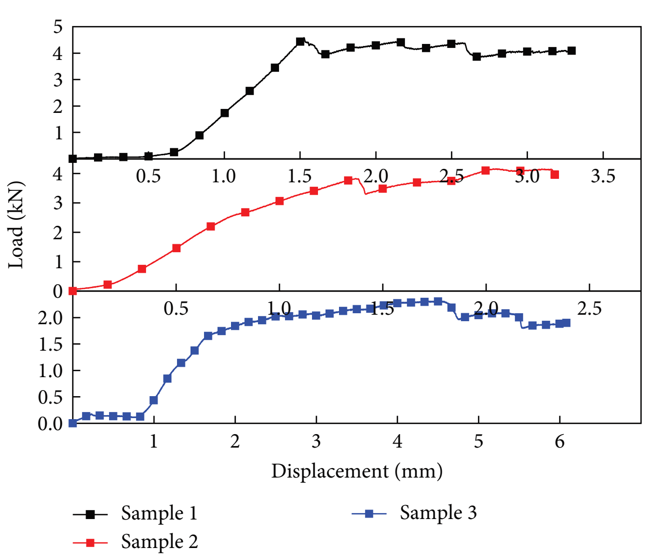

(e)

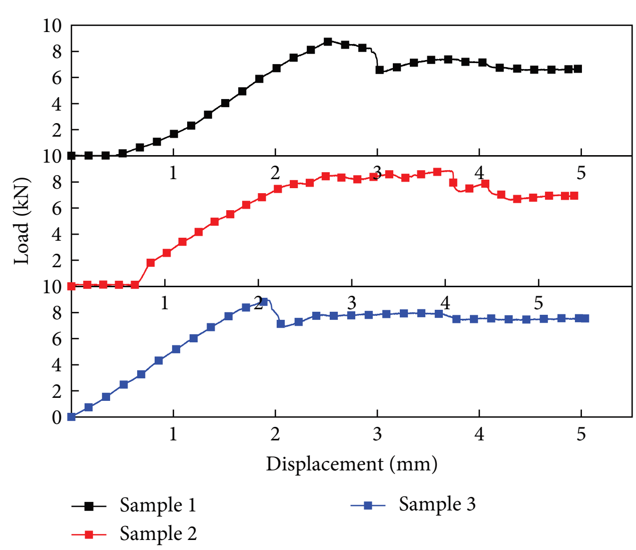

(f)

FIGURE 6: Continued.

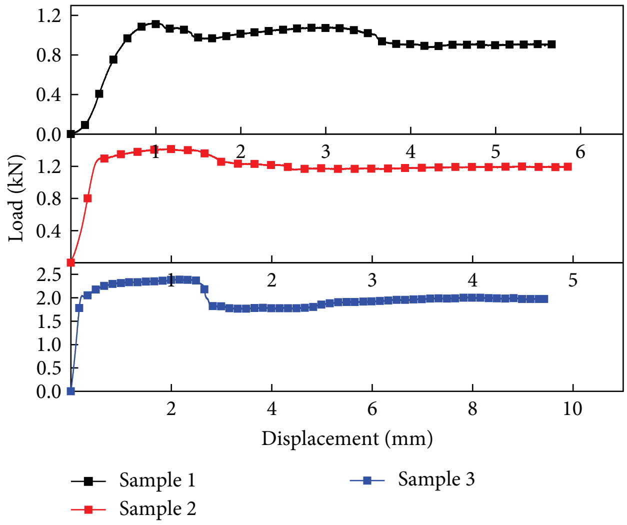

(g)

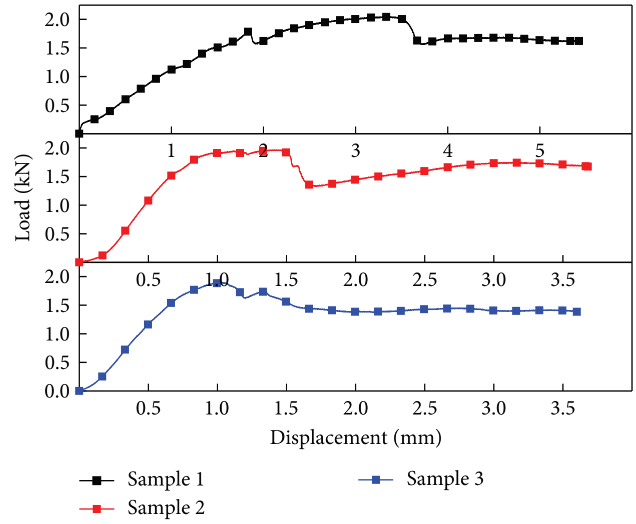

(h)

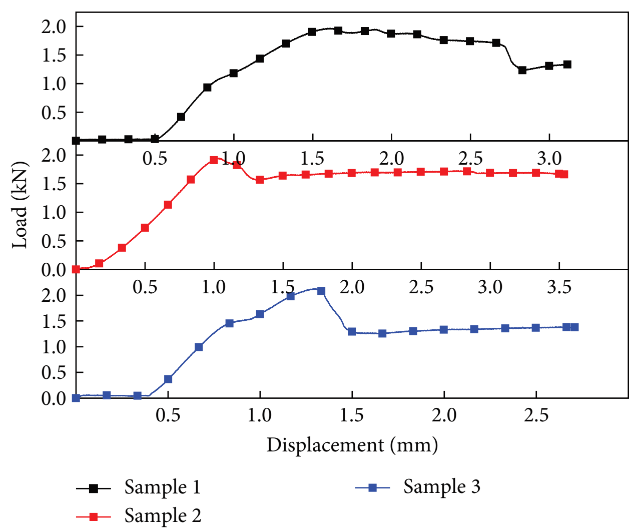

(i)

FIGURE 6: 1d load–displacement curves of foam concrete prepared by various groups in orthogonal experiments. (a) The 1st group of three specimens. (b) The 2nd group of three specimens. (c) The 3rd group of three specimens. (d) The 4th group of three specimens. (e) The 5th group of three specimens. (f) The 6th group of three specimens. (g) The 7th group of three specimens. (h) The 8th group of three specimens. (i) The 9th group of three specimens.

the increase in load leads to the compression of the surface pores of foam concrete, and the numerous pores within the foam concrete are compacted and filled, leading to a rapid increase in displacement. The compacted stage can be further divided into elastic compaction and brittle compaction. In the elastic compaction stage, the load–displacement curve shows an approximately linear relationship, with displacement linearly increasing with the load. This stage is mainly borne by the cement matrix after the initial compaction stage. In the brittle compaction stage, the displacement shows a temporary downward trend with the increase in load. This phenomenon occurs because the residual pores inside the concrete continue to collapse under the load, causing a brief non-dense phenomenon, leading to a slight decrease in load. As the load continues to act, the pores will be compressed, and the load will increase until reaching the peak. In the yield stage, the specimen undergoes plastic deformation, which means that the displacement increases significantly while the load increments relatively smaller. The load–displacement curve begins to drop sharply, showing nonlinear characteristics. Meanwhile, the foam concrete specimen starts to develop numerous cracks. However, compared to the rapid brittle failure of ordinary concrete, the pore structure of foam concrete provides it with good cushioning ability, preventing rapid fracture. Subsequently, the platform stage is entered, during which the load–displacement curve tends to be flat. This means that the displacement continues to increase while the load remains constant until the loading is stopped. The reason is that the foam concrete continues to be compressed under the action of the load, leading to the destruction of the

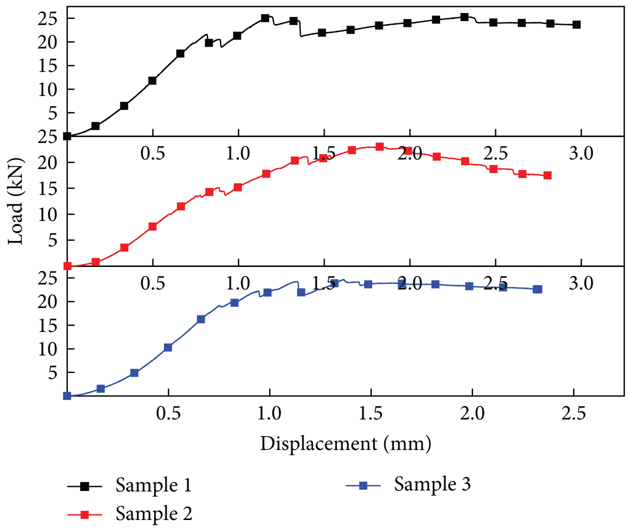

(a)

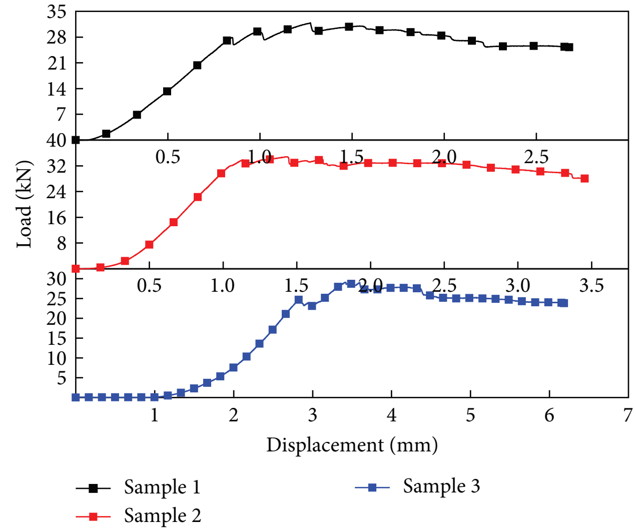

(b)

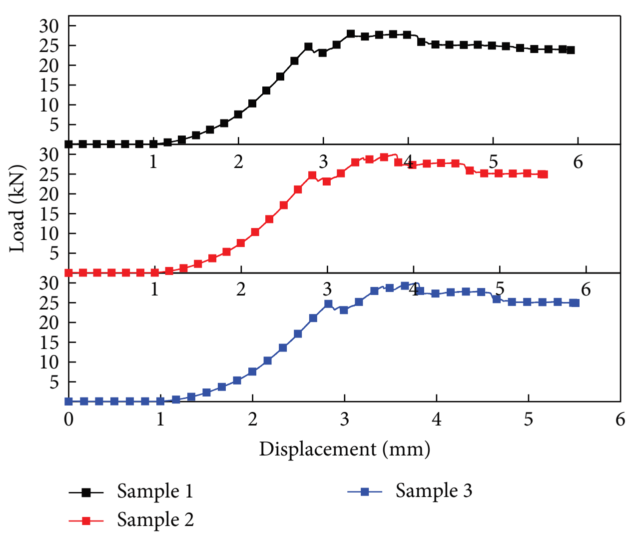

(c)

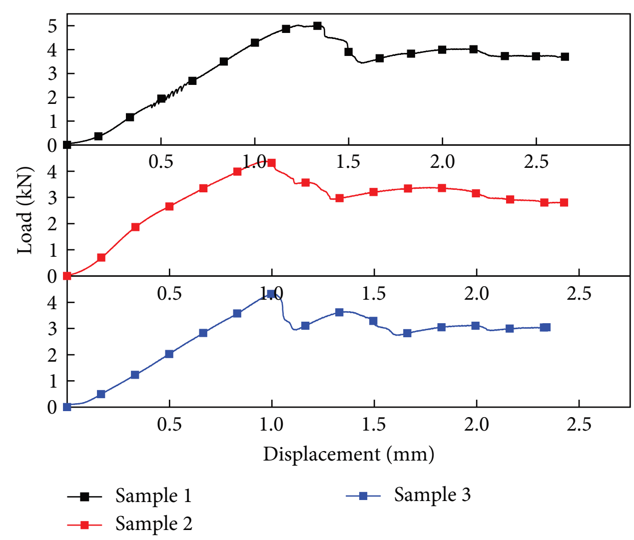

(d)

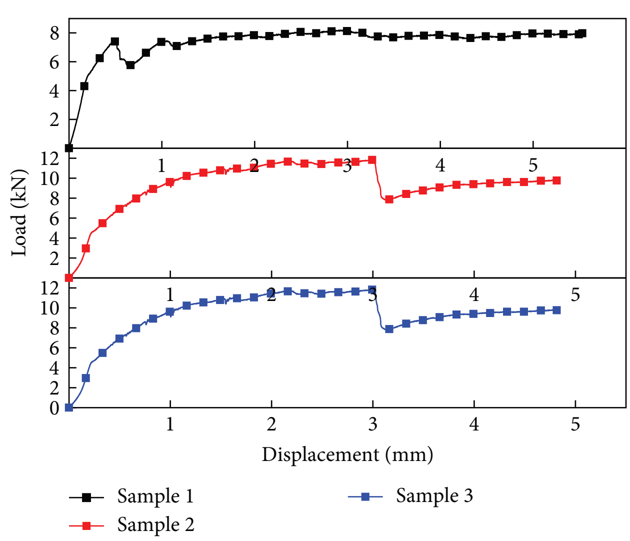

(e)

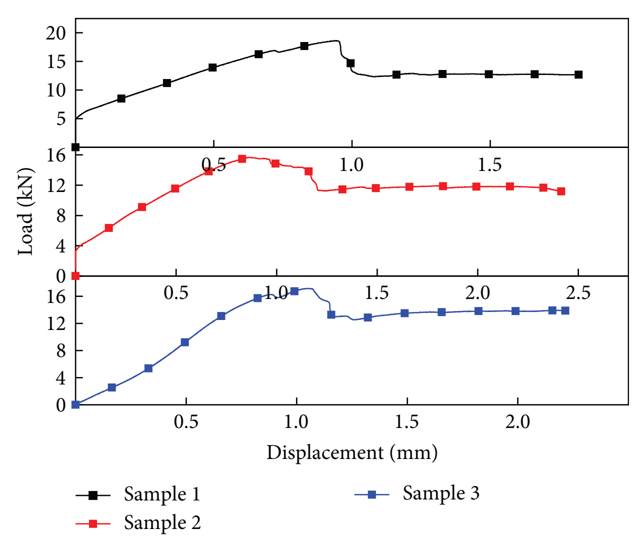

(f)

Figure 7: Continued.

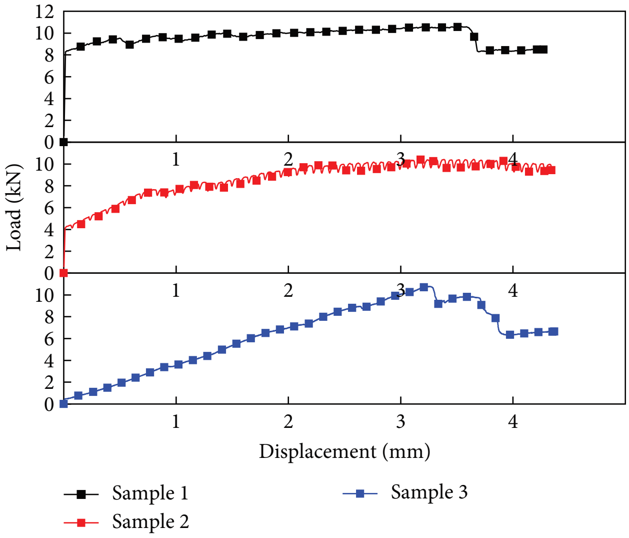

(g)

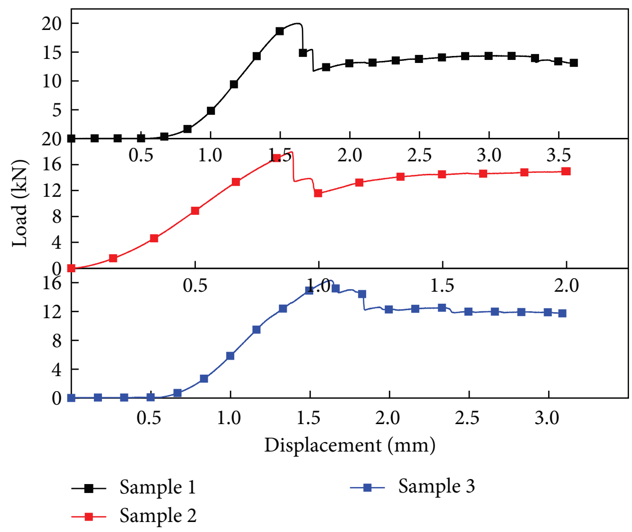

(h)

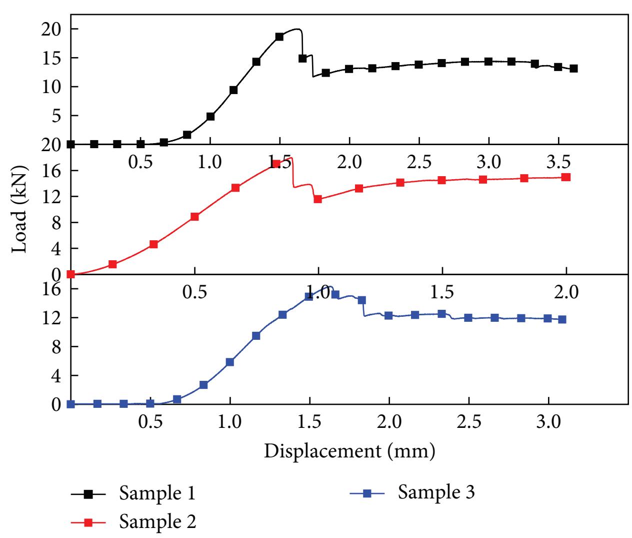

(i)

Figure 7: 3d load–displacement curves of foam concrete prepared by various groups in orthogonal experiments. (a) The 1st group of three specimens. (b) The 2nd group of three specimens. (c) The 3rd group of three specimens. (d) The 4th group of three specimens. (e) The 5th group of three specimens. (f) The 6th group of three specimens. (g) The 7th group of three specimens. (h) The 8th group of three specimens. (i) The 9th group of three specimens.

Table 3: Strength index test results of rapid-hardening foam concrete under uniaxial compression.

Test number	α	β	γ	δ	1d compressive strength (MPa)	3d compressive strength (MPa)
1	100	3.8	0.5	0.1	1.7054	2.4448
2	100	4.0	0.55	0.12	2.5471	3.1915
3	100	4.2	0.6	0.14	2.1963	2.8145
4	50	3.8	0.55	0.14	0.851	0.5013
5	50	4.0	0.6	0.1	0.3685	0.4574
6	50	4.2	0.5	0.12	0.8869	1.0018
7	0	3.8	0.6	0.12	0.1645	1.0604
8	0	4.0	0.5	0.14	0.1972	1.7154
9	0	4.2	0.55	0.1	0.202	1.8099

Table 4: Orthogonal experiment, each group with three specimens, 1-day compressive strength error percentage.

Test number	Specimen 1 Compressive strength (MPa)	Specimen 2 Compressive strength (MPa)	Specimen 3 Compressive strength (MPa)	Average compressive strength (MPa)	Percentage of error between specimen 1 and average (%)	Percentage of error between specimen 2 and average (%)	Percentage of error between specimen 3 and average (%)
1	1.8177	1.6437	1.6548	1.7054	6.6	3.6	3.0
2	2.5411	2.7990	2.3011	2.5471	0.2	9.9	9.7
3	2.2969	2.2929	1.9991	2.1963	4.5	4.4	9.0
4	0.8513	0.8531	0.8504	0.8510	0.0	0.2	0.0
5	0.2314	0.4581	0.4159	0.3685	37	24%	13
6	0.8781	0.8865	0.8960	0.8869	0.9	0.0	1.0
7	0.1120	0.1416	0.2397	0.1645	32	14	46
8	2.0474	1.9692	1.8988	1.9718	3.8	0.1	3.7
9	1.9687	1.9687	2.1232	2.0202	2.5	2.5	5.1

Table 5: Orthogonal experiment, each group with three specimens, 3-day compressive strength error percentage.

Test number	Specimen 1 Compressive strength (MPa)	Specimen 2 Compressive strength (MPa)	Specimen 3 Compressive strength (MPa)	Average compressive strength (MPa)	Percentage of error between specimen 1 and average (%)	Percentage of error between specimen 2 and average (%)	Percentage of error between specimen 3 and average (%)
1	2.5411	2.3248	2.4685	2.4448	3.9	4.9	1.0
2	3.1915	3.4814	2.9016	3.1915	0.0	9.1	9.1
3	2.8114	2.8160	2.8160	2.8145	0.1	0.0	0.0
4	0.3701	0.5502	0.5836	0.5013	26	9.8	16
5	0.5021	0.4383	0.4318	0.4574	9.8	4.2	5.6
6	0.8869	0.8200	1.1836	1.0018	11	18	18
7	1.0592	1.0449	1.0770	1.0604	0.1	1.5	1.6
8	1.8627	1.5668	1.7168	1.7154	8.6	8.7	0.0
9	1.9988	1.7971	1.6337	1.8099	10	0.7	9.7

pore structure, and the pores close up, increasing the axial deformation of the specimen. Additionally, the bearing capacity remains relatively high during this stage. This result indicates that after yielding, foam concrete still possesses a certain load-bearing capacity and buffering performance.

The experimental results in Table 3 indicate that the 1-day compressive strength of foam concrete prepared with 100% rapid-hardening calcium aluminate cement is significantly higher than that of foam concrete prepared with 50% rapid-hardening calcium aluminate cement and foam concrete prepared with ordinary silicate cement. This suggests that the inclusion of rapid-hardening calcium aluminate cement plays a crucial role in enhancing the early compressive strength of foam concrete. The maximum compressive strength of foam concrete prepared with 100% rapid-hardening calcium aluminate cement in 1 day can reach 2.5471 MPa, even higher than the compressive strength of foam concrete prepared with ordinary silicate cement and the compressive strength of foam concrete prepared with a combination of the two at 3 days. The maximum compressive strength of foam concrete prepared with 100% rapid-hardening calcium aluminate cement at 1 day is 13 times that of the maximum compressive strength of foam concrete prepared with ordinary silicate cement at 1 day, and it is 3 times that of the maximum compressive strength of foam concrete prepared with a combination of the two at 1 day. Furthermore, the maximum compressive strength of foam concrete prepared with 100% rapid-hardening calcium aluminate cement at 3 days can reach 3.1915 MPa, which is 3 times the maximum compressive strength of foam concrete prepared with ordinary silicate cement at 3 days and 2 times the maximum compressive strength of foam concrete prepared with a combination of the two at 3 days. The results indicate that rapid-hardening calcium aluminate cement significantly enhances the 1-day compressive strength of foam concrete, but its effect on the 3-day compressive strength of foam concrete is not significant, and in some cases, the 3-day compressive strength of foam concrete prepared with a combination of the two is even lower than that of foam concrete prepared with ordinary silicate cement.

3.3. Sensitivity Range Analysis of Each Factor. The intuitive analysis method examines the problem by analyzing the range of each factor to explore the extent to which different levels of each factor affect the indicator [18]. A smaller range indicates that the differences between the different levels of the factors are smaller, indicating that these factors are not significant and do not significantly affect the experimental results.

Table 6: Analysis of variance results.

Target parameter	Range calculation	α	β	γ	δ
1d compressive strength	K1	2.1496	0.9070	0.9298	0.7586
	K2	0.7021	1.0376	1.2000	1.1995
	K3	0.1879	1.0951	0.9098	1.0815
	R	1.9617	0.1881	0.2903	0.4409
3d compressive strength	K1	2.8169	1.3355	1.7207	1.5707
	K2	0.6535	1.7881	1.8342	1.7512
	K3	1.5286	1.8754	1.4441	1.6771
	R	2.1634	0.5399	0.3901	0.1805

Sensitivity analysis refers to the quantitative analysis of variations in factors that affect the achievement of objectives to determine the impact and sensitivity of these factor changes on achieving the objectives [18]. In optimization problems, sensitivity analysis can help identify which parameters' variations have the greatest impact on the optimization objective, providing guidance in the optimization process. Sensitivity analysis was conducted on the compressive strength test data of foam concrete specimens at different levels of each factor in Table 3, and the sensitivity analysis results are shown in Table 6. In addition, Table 6 shows the summation of indicators for quick-setting sulfoaluminate cement dosage, foam dosage, water-cement ratio, and superplasticizer dosage under Factor 1 levels (K1), under Factor 2 levels (K2), and Factor 3 levels (K3).

As shown in Table 6, the 1-day compressive strength of foamed concrete is influenced by four factors as follows: Rapid-hardening sulfoaluminate cement (α) > Superplasticizer content (δ) > Foam content (β) > Water-cement ratio (γ). The results indicate that factor α (rapid-hardening sulfoaluminate cement) plays a major role in controlling the 1-day compressive strength, while the effect of the water-cement ratio is not significant. Furthermore, the impact of the four factors on the 3-day compressive strength of foamed concrete is ranked as follows: Rapid-hardening sulfoaluminate cement (α) > Water-cement ratio (γ) > Foam content (β) > Superplasticizer content (δ). The study shows that factor α (rapid-hardening sulfoaluminate cement) also plays a major role in controlling the 3-day compressive strength, while the influence of the superplasticizer is not significant.

To more intuitively analyze the influence of various factors on the 1d and 3d compressive strength of foam concrete, an intuitionistic analysis chart of the influence of various factors on the compressive strength is drawn according to the range analysis results in Table 6, as shown in Figure 8. From Figure 8, it can be observed that with an increase in the content of rapid-hardening sulfoaluminate cement, the compressive strength of foam concrete specimens at 1-day increases. When the content of rapid-hardening sulfoaluminate cement increases from 0% to 100%, the compressive strength of specimens in 1 day increases tenfold. Furthermore, specimens with 100% rapid-hardening sulfoaluminate cement content exhibit significantly higher 1-day compressive strength compared to other content groups. As for the 3-day compressive strength of foam concrete specimens, it initially decreases and then increases with an increase in the content of rapid-hardening sulfoaluminate cement. However, the overall increase in compressive strength from 1 day to 3 days is not substantial. In summary, the content of rapid-hardening sulfoaluminate cement is the most significant factor affecting the compressive strength at both 1 day and 3 days. With an increase in the foam content, the compressive strength at 1 day and 3 days of the specimens increases. When the foam content increases from 3.8% to 4.2%, the 1-day and 3-day compressive strength of foam concrete increases by 20.7% and 40.4%, respectively. The analysis indicates that foam content is not the most significant factor affecting the 1-day and 3-day compressive strength of foam concrete. When the water-cement ratio increases from 0.5 to 0.6, the 1-day and 3-day compressive strength of foam concrete specimens initially increases and then decreases. When the water-cement ratio is 0.55, the compressive strength reaches its maximum, with increases of 31.9% and 27% for 1 day and 3 days, respectively. The analysis shows that the water-cement ratio is a significant factor affecting the 3-day compressive strength of foam concrete but not the 1-day compressive strength. With an increase in the superplasticizer content from 0.1% to 0.14%, the 1-day and 3-day compressive strength of foam concrete specimens initially increases and then decreases. When the superplasticizer content is 0.12%, the compressive strength reaches its maximum, with an increase of 58.11% for 1 day and 11.49% for 3 days. Data analysis suggests that the superplasticizer content is a significant factor affecting the 1-day compressive strength of foam concrete but not the 3-day compressive strength. Through range analysis, considering the maximum compressive strength of foam concrete specimens at 1 day and 3 days, the optimal mix ratio is determined as $\alpha 1\beta 2\gamma 2\delta 2$, where the rapid-hardening sulfoaluminate cement content is 100%, foam content is 4%, water-cement ratio is 0.55, and superplasticizer content is 0.12%.

3.4. Analysis of Variance of Strength Test Indicators. Based on the test results of foamed concrete strength indicators in Table 3, a variance analysis was conducted to investigate whether various factors have a significant influence on the 1-day and 3-day compressive strength and to identify the main influencing factors of foamed concrete strength

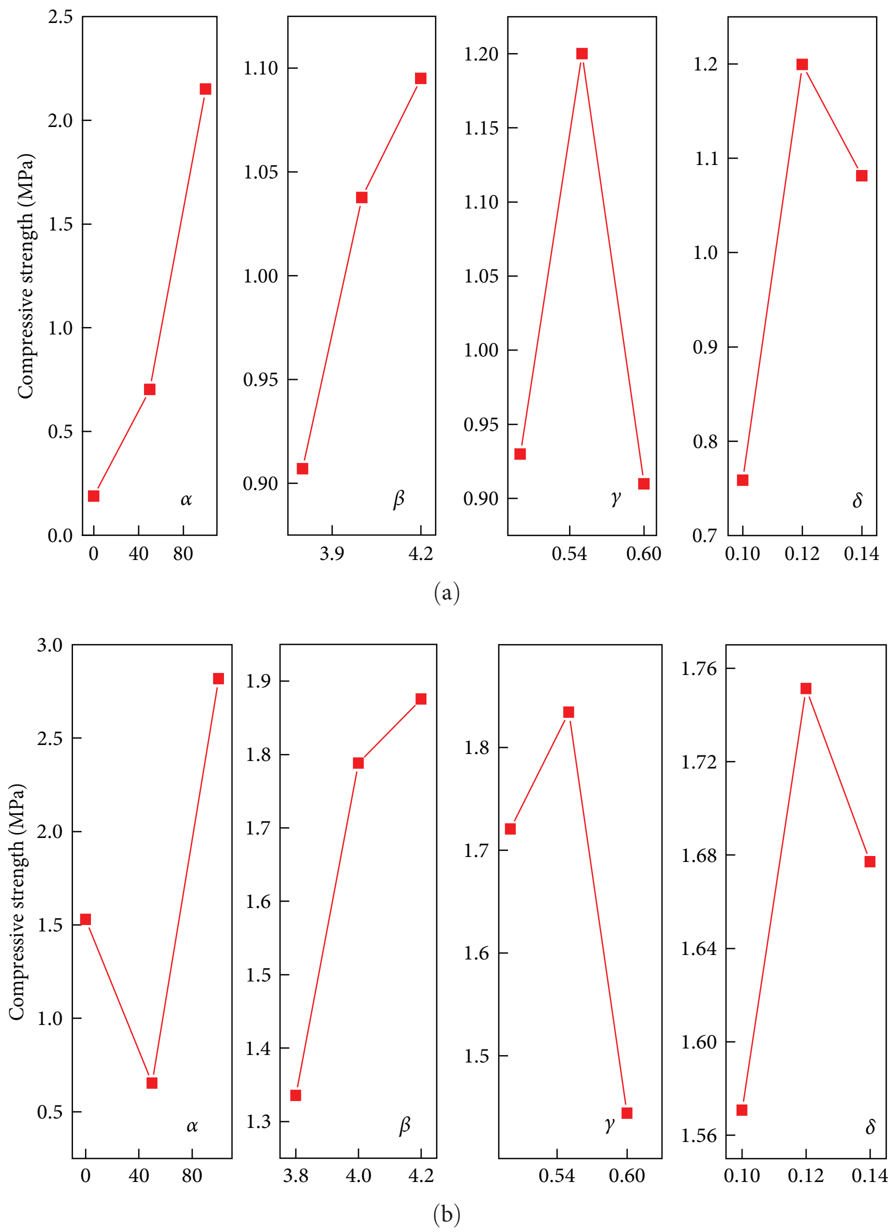

Figure 8: The influence of four factors on the compressive strength of 1 day and 3 days. (a) 1d compressive strength. (b) 3d compressive strength.

indicators. The variance analysis results of the foamed concrete strength indicators are recorded in Table 7.

The variance analysis results presented in Table 7 reveal the significance of various factors when considering the 1-day and 3-day compressive strength of foamed concrete. For the 1-day compressive strength, the significance levels (p-values) for the content of rapid-hardening sulfoaluminate cement (α), foam content (β), water-cement ratio (γ), and superplasticizer content (δ) are all below 0.05, indicating that these factors significantly influence the 1-day compressive strength of foamed concrete. Additionally, the statistical analysis of significance levels, as shown in Figure 9, visually demonstrates that among these factors, the content of rapid-hardening sulfoaluminate cement (α) has the smallest p-value, indicating it is the most significant influencing factor, while the foam content (β) has the highest p-value, suggesting its influence is relatively weaker. Similarly, for the 3-day compressive strength, the significance levels (p-values) of these four factors are also below 0.05, showing they significantly affect the 3-day compressive strength of foamed concrete. The statistical analysis of significance levels, as depicted in Figure 9, clearly illustrates that among these factors, the content of rapid-hardening sulfoaluminate cement (α) consistently has the smallest p-value, further confirming its status as a highly significant influencing factor, whereas the superplasticizer content (δ) has a relatively larger p-value, indicating its influence is comparatively weaker.

Table 7: Results of analysis of variance.

Target parameter	Source of variation	Sum of squares	Degrees of freedom	Mean square	F-value	Significance level (p)
1d compressive strength (MPa)	α	6.2079	2	3.1039	6.99×10^{15}	1.43×10^{-16}
	β	0.0558	2	0.0279	6.28×10^{13}	1.59×10^{-14}
	γ	0.1577	2	0.0788	1.78×10^{14}	5.63×10^{-15}
	δ	0.3125	2	0.1563	3.52×10^{14}	2.84×10^{-15}
3d compressive strength (MPa)	α	7.1061	2	3.5530	1.43×10^{14}	7.00×10^{-15}
	β	0.5040	2	0.2520	1.01×10^{13}	9.87×10^{-14}
	γ	0.2416	2	0.1208	4.86×10^{12}	2.06×10^{-13}
	δ	0.0494	2	0.0247	9.93×10^{11}	1.01×10^{-12}

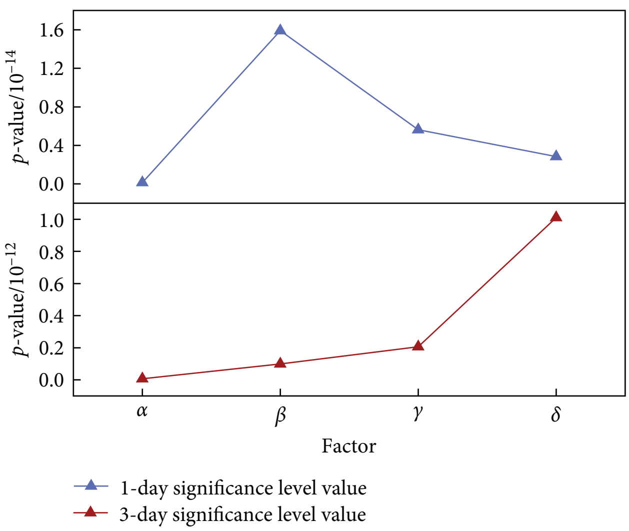

Figure 9: Significance levels of different factors affecting compressive strength.

The variance analysis shows that the smaller the significance level (p-value), the greater the impact of a factor on the target variable. The main and secondary order of the influence of each factor on the 1-day compressive strength of foamed concrete specimens is as follows: rapid-hardening sulfoaluminate cement (α) > Superplasticizer content (δ) > Foam content (β) > Water-cement ratio (γ). Similarly, for the 3-day compressive strength of foamed concrete specimens, the main and secondary order of influence for each factor is rapid-hardening sulfoaluminate cement (α) > Water-cement ratio (γ) > Foam content (β) > Superplasticizer content (δ).

By using both variance analysis and range analysis methods, the most reliable optimal mix ratio for maximizing the 1-day and 3-day compressive strength of foamed concrete specimens is determined to be $\alpha1\beta2\gamma2\delta2$, which means a rapid-hardening sulfoaluminate cement content of 100%, foam content of 4%, water-cement ratio of 0.55, and superplasticizer content of 0.12%.

4. Conclusions

Based on the above, the following conclusions were drawn that can be used as practical guidance for the preparation of rapid-hardening foam concrete.

(1) The load–displacement curves of foamed concrete prepared under the influence of the four factors exhibit distinct stages. Through the analysis of the load–displacement curves, the compressive process of foamed concrete can be divided into four stages: initial densification stage, densification stage, yielding stage, and plateau stage. Each stage shows different characteristics and reasons for the observed behavior. By conducting a stage-by-stage analysis of load–displacement curves, a deeper understanding of the fracture mechanism of foam concrete materials can be obtained, while also providing a theoretical and experimental foundation for a more in-depth analysis of the impact of the four factors on foam concrete performance.

(2) Using the range analysis method to reflect the impact of different levels of each factor on the indicators, it is found that the sensitivity of the four factors to the 1-day compressive strength of foamed concrete specimens is as follows: Fast-hardening sulfoaluminate cement (A) > Superplasticizer content (D) > Foam content (B) > Water-cement ratio (C). Similarly, the impact of the four factors on the 3-day compressive strength is ranked as follows: Fast-hardening sulfoaluminate cement (A) > Water-cement ratio (C) > Foam content (B) > Superplasticizer content (D). The optimal mix ratio obtained through range analysis is A1B2C2D2, which involves using 100% fast-hardening sulfoaluminate cement, 4% foam content, 0.55 water-cement ratio, and 0.12% superplasticizer content.

(3) Using the variance analysis method to assess the significance levels of each factor, it is determined that all four factors significantly influence the 1-day compressive strength of foamed concrete specimens. Fast-hardening sulfoaluminate cement is a highly significant influencing factor, while the foam content has the weakest impact. Moreover, all four factors are found to significantly influence the 3-day compressive strength of foamed concrete specimens, with fast-hardening sulfoaluminate cement being the most significant factor and superplasticizer content having the weakest effect. Furthermore, the main and secondary orders of influence of each factor on the 1-day compressive strength of foamed concrete are Fast-hardening sulfoaluminate cement

(A) > Superplasticizer content (D) > Foam content (B) > Water-cement ratio (C). Similarly, for the 3-day compressive strength, the order of influence is Fast-hardening sulfoaluminate cement (A) > Water-cement ratio (C) > Foam content (B) > Superplasticizer content (D). The optimal mixing ratio obtained through the analysis of variance method is consistent with the results obtained from the range analysis method, which is A1B2C2D2 as the optimal mixing ratio.

(4) Using the range analysis method and variance analysis method, we can rank the significance of each factor, determining the degree of influence of each factor and identifying the optimal mix ratios for various materials when considering 1-day and 3-day compressive strength. Determining the significance of each factor and the optimal mix ratios can play a crucial role in rapid repair and construction projects. It enables the precise and rapid use of materials with the greatest impact and optimal mix ratios for preparing foam concrete, facilitating quick repairs. Additionally, for materials with less significant impact, their omission during the application process can result in material savings without compromising repair effectiveness.

Data Availability

Some or all data, models, or codes that support the findings of this study are available from the corresponding author upon reasonable request (list items).

Conflicts of Interest

The authors declare that they have no conflicts of interest.

Authors' Contributions

Experiment: X. Z. and R. Y.; writing: Y. L., D. Z., and J. X.; processing data: Q. L. and W. Q.; all authors have read and agreed to the published version of the manuscript.

Acknowledgments

This research was funded by Key Research and Development Projects of Shaanxi Province (2024GX-YBXM-372, 2023KXJ-159, and 2024QCY-KXJ-176); Department of Transport of Shaanxi Province (22-38K and 23-39R); The Natural Science Foundation of Shaanxi Province (2021JM-165); Innovation Capability Support Program of Shaanxi (2023-CX-TD-35).

References

[1] D. Briskorn, A. Kimms, and D. Olschok, "Simultaneous planning for disaster road clearance and distribution of relief goods: a basic model and an exact solution method," *OR Spectrum*, vol. 42, no. 3, pp. 591–619, 2020.

[2] C. T. Liu, "Study on the preparation and performance of fast-hardening and high-strength foamed concrete," Chongqing Jiaotong University, 2021.

[3] W. K. Zheng, Y. H. Zhao, Y. C. Wang, and H. Li, "The simulation study on static mixer for foamed concrete preparation," *Materials Reports*, vol. 38, no. 15, Article ID 23010061, 2023.

[4] X. Yuanliang, L. Baoliang, C. Chun, and Z. Yamei, "Properties of foamed concrete with $Ca(OH)_2$ as foam stabilizer," *Cement and Concrete Composites*, vol. 118, no. 6, Article ID 103985, 2021.

[5] J. T. Dang, X. S. Tang, J. Z. Xiao, Z. H. Duan, and A. H. Han, "Early stability behavior and mechanism of alkali-activated foamed concrete," *Journal of Building Materials*, vol. 26, no. 7, pp. 746–754, 2023.

[6] Y. J. Li, S. Wang, S. K. Zhang, and D. Z. Feng, "Preparation and deformation characterization of carbon nanotube-reinforced fly ash foamed concrete," *Journal of Yangtze River Scientific Research Institute*, pp. 1–10, 2023.

[7] Y. H. Hao, H. Sun, L. D. Qin, Z. X. Wu, T. Y. Ci, and X. M. Guo, "Experiment on mix ratio of fly ash foamed concrete reinforced by micro aggregate," *Journal of Functional Materials*, vol. 53, no. 10, pp. 10229–10236, 2022.

[8] M. Xiao, F. Li, P. Yang, B. Li, J. Wei, and Q. Yu, "Influence of slurry characteristics on the bubble stability in foamed concrete," *Journal of Building Engineering*, vol. 71, pp. 2352–7102, 2023.

[9] Z. H. Gao, B. Chen, J. L. Chen, and Z. Y. Yuan, "Pore structure and mechanical properties of foam concrete under freeze-thaw environment," *Acta Materiae Compositae Sinica*, vol. 41, pp. 1–12, 2023.

[10] H. Liu, H. Y. Zhou, X. J. Wang, and H. Zhang, "In-plane compression properties of negative Poisson's ratio structure of rotating thin-walled multi-cell square tubes with foam concrete filler," *Acta Materiae Compositae Sinica*, vol. 41, pp. 1–19, 2023.

[11] Z. H. Liu, X. D. Chen, Y. J. Ning, and J. J. Wang, "Experimental investigation on the mechanical properties of thefoamed con-crete with thermal treatment under triaxial compression," *Journal of Central South University (Science and Technology)*, vol. 54, no. 4, pp. 1552–1561, 2023.

[12] O. Gencel, M. Nodehi, O. Y. Bayraktar et al., "Basalt fiber-reinforced foam concrete containing silica fume: an experimental study," *Construction and Building Materials*, vol. 326, 2022.

[13] C. Ma and B. Chen, "Properties of foamed concrete containing water repellents," *Construction and Building Materials*, vol. 123, pp. 106–114, 2016.

[14] T. Li, F. M. Huang, L. Li, J. Zhu, X. Jiang, and Y. B. Huang, "Preparation and properties of sulphoaluminate cement-based foamed concrete with high performance," *Construction and Building Materials*, vol. 263, 2020.

[15] A. J. Ashfaque, I. G. Wan, K. M. Aamir, F. T. Abdoul, and O. Mahboob, "Environmental assessment and mechanical properties of Polypropylenefibres reinforced ternary binder foamed concrete," *Environmental Science and Pollution Research International*, vol. 29, no. 2, pp. 1–23, 2021.

[16] R. Tang, Q. S. Wei, K. Zhang et al., "Preparation and performance analysis of recycled PET fiber reinforced recycled foamed concrete," *Journal of Building Engineering*, vol. 57, 2022.

[17] M. Y. Hang and R. Yang, "Influence of mineral admixtures on properties of foam concrete," *Bulletin of the Chinese Ceramic Society*, vol. 37, no. 4, pp. 1480–1486, 2018.

[18] J. Y. Dong, J. H. Yang, G. X. Yang, and F. Q. Wu, "Research on similar material proportioning test of model test based on or-thogonal design," *Journal of China Coal Society*, vol. 37, no. 1, pp. 44–49, 2012.

[19] J. S. Zhang, *Foam Concrete*, Harbin Institute of Technology Press, Harbin, 2016.

[20] Z. Y. Yuan, B. Chen, J. L. Chen, and Z. H. Gao, "Characterization of pore structure of foamed concrete and its influence on per-formance," *Acta Materiae Compositae Sinica*, vol. 40, no. 7, pp. 4117–4127, 2023.

[21] C. T. Zhou, B. Chen, and Z. H. Gao, "Uniaxial compression characteristics of foamed concrete under freeze-thaw environment," *Bulletin of the Chinese Ceramic Society*, vol. 42, no. 4, pp. 1233–1241, 2023.